Tuning the affinity of tandem calponin homology domains

Andrew R Harris[1], Brian Belardi[1], Pamela Jreij[1], Kathy Wei[1], Andreas Bausch[3], Daniel A Fletcher[1,2,4]*

Affiliations

[1]Department of Bioengineering and Biophysics Program, University of California, Berkeley, 648 Stanley Hall MC 1762, Berkeley, CA 94720, USA

[2]Biological Systems and Engineering Division, Lawrence Berkeley National Laboratory, 648 Stanley Hall MC 1762, Berkeley, CA 94720, USA

[3]Lehrstuhl für Biophysik (E27), Technische Universität München, Garching 85748, Germany.

[4]Chan Zuckerberg Biohub, San Francisco, CA 94158

*Daniel A Fletcher, fletch@berkeley.edu

Abstract

Tandem calponin homology (CH) domains are common actin-binding motifs found in proteins such as α-actinin, filamin, utrophin, and dystrophin that organize actin filaments into functional structures. Despite a conserved structural fold and regions of high sequence similarity, different tandem calponin homology (CH1-CH2) domains have remarkably different actin-binding properties. Point mutations to tandem CH domains arise in a number of pathologies and can result in both gain-of-function (increased affinity for f-actin) and loss-of-function (decreased affinity for f-actin) phenotypes. How such subtle variations in CH1-CH2 sequence affect binding affinity is poorly understood. By examining naturally occurring variations in CH1-CH2 domains and using site-directed mutagenesis, we show that changes to the inter-CH domain interface and linker region lead to an increasingly 'open' configuration of the two CH domains and result in increased affinity, while an increasingly 'closed' configuration result in decreased affinity for filamentous actin. The increase in affinity of the 'open' configuration can be reversed by increasing the physical size of the CH2 domain, presenting a potential therapeutic strategy for gain-of-function diseases. Interestingly, we observed changes in sub-cellular localization of tandem CH domains to different actin structures that are independent of actin-binding affinity, but dependent on the n-terminal unstructured region prior to CH1. This sequence-dependent separability of affinity and localization has implications for interpretation of disease-associated mutations and engineering actin-binding domains with specific properties.

The actin cytoskeleton is organized and regulated by the interaction of actin filaments with a wide range of ancillary proteins(1, 2). Tandem calponin homology (CH1-CH2) domains are common actin-binding motifs found in diverse proteins, including the actin crosslinkers, α-actinin and filamin, as well as the membrane-actin linkers, utrophin and dystrophin(3, 4). CH1-CH2 domains are composed of a type 1 and a type 2 calponin homology (CH) domain, which each consist of a conserved structural fold of four alpha helices(4). CH1-CH2 domains contain three regions that have been proposed to interface to f-actin, named actin-binding surface (ABS) 1, 2, and 3(4) (Fig 1A). Despite regions of high sequence conservation (~20% identity and ~30% conservation across the tandem domain (Fig S1)) and a conserved structural fold (5), different CH1-CH2 domains have binding affinities for filamentous actin that vary by an order of magnitude. For example, the affinity of α-actinin-1 is reported to be 4μM(6), while the affinity of α-actinin-4's actin-binding domain is >50μM(7). Similarly, the affinity of the actin-binding domain of filamin A is 47μM(8), while the affinity of filamin B is 7μM (9). The affinity of utrophin's actin-binding domain is 19μM, while the affinity of its muscle homologue dystrophin is 44μM(6).

The ability for small differences in domain sequence to have a significant impact on f-actin affinity is particularly clear in disease-associated CH1-CH2 mutations. Mutations to the tandem calponin homology domain of α-actinin-4 result in kidney disorders (10, 11) (Focal Segmental Glomerulosclerosis), while those in filamin isoforms and dystrophin cause skeletal(12, 13) (Skeletal Dysplasia) as well as migratory disorders(14) (Periventricular Nodular Heterotopia) and Muscular Dystrophy(15). Interestingly, many of these diseases arise from single point mutations that can result in either loss-of-function (decreased affinity for filamentous actin) or gain-of-function (increased affinity for filamentous actin). For example, the K255E mutation in α-actinin-4 at least doubles the actin-binding affinity(7), and the M251T mutation in filamin C reduces the binding affinity by half(16). Such increases in actin-binding affinity can cause excessive bundling and crosslinking of the cytoskeleton, compromising cellular function(10, 17) and result in changes to the mechanical and dynamical characteristics of the cytoskeleton(1, 18–20). This suggests that precise tuning of CH1-CH2 affinity for filamentous actin may be critical for homeostasis of the actin cytoskeleton.

Here, we use natural variations in wild-type tandem calponin homology domains and site-specific mutations to show that CH1-CH2 domain affinity can be both increased and decreased by mutations at the CH1-CH2 interface and interdomain linker regions, resulting in tandem calponin homology domains that vary from a 'closed' to 'open' conformation (Fig 1B). Interestingly, we identify new residues outside of the previously-identified salt bridge that contribute to this interaction, and we demonstrate that increases in affinity that result from mutations that create an 'open' configuration can be reversed by increasing the size of the CH2 domain, supporting a model in which the CH2 sterically clashes with f-actin to alter CH1-CH2 affinity. In addition to characterizing the mechanisms that contribute to binding affinity, we show that defined regions on the CH1 influence subcellular localization in live cells. These findings, which are based on a combination of live cell microscopy, in vitro biochemistry, and structural methods, point to previously unappreciated mechanisms that govern the overall binding affinity and selectivity of tandem CH domains despite their high

sequence homology. The ability of small sequence changes in CH1-CH2 domains to tune affinity and sub-cellular localization provides new insight into cytoskeletal organization and regulation by actin-binding proteins and disease-associated mutants.

Results and Discussion

Differences in relative affinity of CH1-CH2 for actin can be detected in live cells

By definition, changes in the affinity of actin-binding proteins for actin will result in different amounts of protein bound to filamentous actin for a given initial solution concentration. We sought to characterize the binding of CH1-CH2 domains i) *in vitro* using traditional co-sedimentation assays and ii) in a cellular context through the relative fraction of protein bound to the cytoskeleton. To characterize the bound fraction of protein in live cells, we developed a custom image analysis approach. The actin cytoskeleton was imaged by expressing the actin-binding domain of utrophin (a common actin-binding label known to only bind to f-actin(21)) fused to EGFP. In a second image channel, the actin-binding domain of interest fused to mCherry was imaged (e.g. the actin-binding domain of filamin A, Fig 1C). Thresholding the actin channel yielded masks of both actin and cytoplasm which could be used to measure the average amount of mCherry fluorescence signal in the two regions (Fig 1C, materials and methods). Four actin-binding domains analyzed in this way show significant differences (Fig 1D). This measurement of relative bound fraction provides a rapid and convenient way to characterize relative affinity of actin-binding domains to actin filaments in a cellular context, and it also enables identification of differences in sub-cellular localization to specific actin structures, if any were present. We used this approach, together with *in vitro* measurements of binding affinity, secondary structure, and size, to determine how sequence differences in CH1-CH2 domains cause different binding behaviors.

The main affinity of CH1-CH2 domains for actin has been proposed to come from the CH1 domain(22), with the CH2 domain playing a regulatory role, endowing solubility and stability(23). To verify this was the case in live cells, we expressed the minimal CH1 and CH2 domains from utrophin fused to mCherry (Fig S2). The isolated CH1 domain of utrophin had a high relative bound fraction (0.55±0.09, p***<0.05 (Fig 1D)), but appeared insoluble, aggregating within cells (Fig S2 A,B), consistent with observations about its stability in vitro(22). The isolated CH2 domain was soluble but distributed throughout the cytosol (Fig S2 C) with a low relative bound fraction (-0.27±0.06, p****<0.05 (Fig 1D), implying that it alone has minimal actin-binding activity. In one model, the CH2 is thought to act as a negative regulator of f-actin-binding through a steric clash with the actin filament upon engagement of the CH1 with f-actin(23). In order to bind with high affinity, the CH1-CH2 conformation must be in an ‘open’ rather than a ‘closed’ conformation(24), where the steric interaction of the CH2 with f-actin is reduced. Native tandem CH domains have been shown to crystalize in a range of different conformations, including ‘open’ for utrophin actin-binding domain (utrophin’s ABD) (1QAG(25), Fig 1B) and ‘closed’ for plectin’s ABD (1MB8(26), Fig

1B). We used relative bound fraction measurements to compare the binding of the minimal CH1-CH2 domains from three native actin-binding proteins, utrophin (Fig S2 D), filamin A (Fig S2 E) and plectin (Fig S2 F), in live cells. Between these three domains, utrophin had the highest relative bound fraction (0.81±0.02, Fig 1D), while plectin had the lowest (-0.09±0.05, p**<0.05, Fig 1D), characterized by a greater cytoplasmic signal (Fig S2 F). These results are consistent with the notion that utrophin resides in a 'open' conformation, while plectin resides in a more 'closed' conformation, with filamin existing between these two(23, 26, 27) and that the conformation of the domains affects binding affinity. Overall, measurements of relative bound fraction correlated well with *in vitro* affinity measurements for the domains that we tested (Fig 1E).

Binding affinity dependence on an inter-CH domain salt-bridge is consistent with an 'open' and 'closed' model of CH1-CH2 domains

Inter-CH domain interactions, specifically a key salt bridge – typically an interaction between an aromatic residue, e.g. tryptophan, on the CH1 and a lysine on the CH2 domain - are predicted to modulate the open-closed conformation of the domain and hence binding affinity(28). Disruption of this salt bridge occurs in gain-of-function actin-binding in diseases such as Focal Segmental Glomerulosclerosis(10) and skeletal dysplasia(12). Since this interaction is highly conserved across CH domains, we sought to test whether it served as a general mechanism governing affinity to f-actin. To test whether changing CH1-CH2 interactions through the conserved salt bridge could increase binding affinity, we made mutations to the CH2 domain targeting residues of the salt bridge for utrophin (K241E, Fig S2 G), filamin A (E254K, Fig S2 H), and plectin (K278E, Fig S2 I) and measured the resulting bound fractions. Consistent with the open and closed model of CH1-CH2 binding, mutations disrupting the inter-domain salt bridge increased the binding of the filamin A (0.64±0.05, p<0.05) and plectin domains (Fig 2A, 0.62±0.03, p**<0.05) to f-actin, resulting in a bound fraction closer to that of utrophin. Furthermore, the same mutation had no effect on the apparent bound fraction of utrophin, consistent with the notion that this domain already exists in an 'open' conformation relative to filamin and plectin (Fig 2A, 0.84±0.02, p=0.08)(27).

To verify these results, we purified and measured the binding affinity of utrophin ABD and plectin ABD in vitro with a co-sedimentation assay (supplementary materials and methods), which had the highest and lowest bound fraction of the three actin-binding domains tested in cells (Fig S3). Utrophin ABD had a significantly higher binding affinity for actin (Fig 2B, Kd=13.8µM) than that of the plectin construct, which showed little binding over the range of actin concentrations that we tested with our assay (Fig 2B Kd≈120µM). Introducing the K278E mutation into plectin, greatly increased its binding affinity in vitro, consistent with a shift towards a relatively more 'open' model of the domain (Fig 2B, Kd=45.1µM). The melting temperature of the purified forms of the tandem CH domain has been used as a proxy for inter-domain interactions and hence conformation (supplementary materials and methods)(22, 29, 30). As expected, the melting temperature of plectin (Tm=64.2°C) was higher than that of utrophin (Tm=57.0°C, Fig 2C), implying a more compact and stable conformation, consistent with a 'closed' CH1-CH2 domain. The plectin K278E mutation had a reduced melting

temperature in comparison to the WT domain (Tm=58.2°C, Fig 2C), suggesting that the domain conformation was in a more 'open' state.

The interdomain linker region and additional inter-CH domain interactions govern ABD compaction and binding affinity

Comparing the sequences of native tandem CH domains, the interdomain linker region appeared to have the highest amount of sequence and structural diversity (Fig S1). It can either be unstructured, in the case of filamin and plectin (not resolved in the crystal structures of filamin A 2WFN(8) or plectin 1MB8(26)), or helical, in the case of utrophin (1QAG(25)) and dystrophin (1DXX(15)). We postulated that the interdomain linker region could have a role in regulating CH domain interactions(31). To test this, we generated chimeras containing the CH1 and CH2 domains from utrophin, but the linker region from filamin A, and examined the bound fraction in live cells (Fig S4). This chimeric protein had a high bound fraction (Fig 3A, 0.80±0.07, p=0.89), implying a high affinity for actin. We expressed and purified this construct and found that the actin-binding affinity *in vitro* was significantly higher than that of WT utrophin actin-binding domain (Kd = 0.7µM, Fig 3B) and that the chimeric protein had a significantly lower melting temperature (Tm = 50.5°C, Fig 3C), indicating a further increase in the 'opening' of the configuration of the tandem CH domain. This indicates that the well-known salt bridge is not the only regulator of the 'open' and 'closed' states and affinity of tandem CH domains.

We next investigated whether additional interactions at the CH-CH interface could further regulate binding affinity. The proposed actin-binding surface 1 (ABS1) is suggested to lie buried between the CH1 and CH2 domains in the closed conformation and become exposed upon domain opening, leading to an increase in actin-binding(10). We introduced the point mutations Q33A and T36A (located within ABS1 on CH1) to the CH1-CH2 domain of utrophin. Surprisingly, the bound fraction of this construct remained high (Fig 3A, 0.87±0.05, p=0.23), implying a high actin-binding affinity. We tested the binding affinity of this construct *in vitro* and observed a significantly higher actin-binding affinity (Kd=0.4µM, Fig 3B) and a lower melting temperature (Tm = 54.9°C, Fig 3C) than WT utrn CH1-CH2. This data suggests that these residues are involved in inter-CH domain interactions, and like changes to the interdomain linker region, can put the CH1-CH2 domains in an increasingly 'open' configuration that is less stable and has a higher affinity than even the WT utrn ABD.

To verify these observations resulted from a change in the conformation of each actin-binding domain, we measured changes in the size and flexibility of these constructs. We measured the radius of gyration (Rg) and the flexibility of the different domains using small angle X-ray scattering (SAXS)(32)(Fig S5, supplementary materials and methods). Consistent with our previous measurements, the plectin construct had the lowest Rg (22Å), suggesting a 'closed' conformation, while the Rg of utrophin was larger (24Å). The utrophin-filamin-linker chimera had the largest Rg (41Å), implying that changing the linker region allowed the domain to adopt a conformation with a large separation between the CH1 and CH2, consistent with a more 'open' state and the large increase in binding affinity. This construct was also the most flexible (Fig S5 E), potentially reducing any steric clash between the CH2 and actin filament upon binding.

The utrn Q33A T36A mutant had a similar Rg to that of utrophin (23.5Å), but was more flexible, consistent with a 'more open' conformation, higher binding affinity and reduced CH2-actin steric clash.

Increased binding affinity of the 'open' configuration can be reversed by increasing the steric contribution of CH2

Having established that the opening of the CH domain regulates actin-binding affinity, we sought to reverse the increases in affinity resulting from mutations that open CH1-CH2 by modifying the CH2 domain, which we have shown is not sufficient for binding actin on its own (Fig S2 C). We hypothesize that opening of the CH1-CH2 domain results in a reduced steric interaction between CH2 and f-actin, providing increased accessibility for CH1 to the f-actin surface. To test whether additional steric constraints could reverse the open conformation's affinity, we increased the size of the CH2 domain by conjugating a small PEG molecule to specific sites on the surface of the domain (Fig 4A). We mutated a serine S158 to cysteine, which was then available for labelling with a maleimide-750Da PEG conjugate, which has an approximate Rg of 1nm. The unconjugated mutant had a similar binding affinity to WT utrn ABD (Kd = 12.5µM). In contrast, the PEG conjugated utrophin ABD had a reduced binding affinity (Kd = 53.8µM). This result highlights that simply increasing the physical size of CH2 can reduce gains in affinity that arise from open conformation domains, supporting the idea that CH2 steric clash with f-actin modulates CH1-CH2 affinity. Interestingly, many disease-associated mutations coincide with an increase in actin-binding affinity. Adding size to the CH2 domain presents a possible therapeutic strategy, for example by a biologic targeted to the CH2 domain, as it could lower the binding affinity of the CH1-CH2 without completely abolishing it and without directly altering the binding surface on the CH1.

Differences in sub-cellular localization are influenced by the n-terminal flanking region and are separable from overall binding affinity

Having found mutations that are involved in the CH1-CH2 interface, we next sought to identify regions on the CH1 domain that contribute directly to the actin-binding interface. Three key regions on the CH1 domain have been reported to be important for affinity to f-actin: ABS2, ABS2-N and the n-terminal flanking region (33, 34). The n-terminal flanking region has both a high degree of sequence diversity as well as different lengths of sequence (Fig 5A) (29, 33, 34). To test the contribution of the n-terminal region to f-actin-binding, we truncated the n-terminal region (residues 1-27) of utrn ABD and expressed the remaining CH1-CH2 domain in live cells (Fig S6 A). This construct (Δ-nterm) was largely cytoplasmic and had a low bound fraction (0.25±0.03, $p<0.05$), implying a low binding affinity to F-actin compared to WT utrn CH1-CH2.

Based on our results showing the effect of inter-CH domain interactions on affinity, we speculated that it should be possible to reverse this loss in binding affinity by modifying the inter-CH domain interface to make the construct even more 'open'. To test this idea, we introduced the ABS1 mutations Q33A T36A (Δ-n-term Q33A T36A), a mutation that we have shown increases the affinity of the WT utrn CH1-CH2 domain

more than 10-fold (Fig 3B). Indeed, this mutation restored the bound fraction of the Δ-n-term to f-actin in live cells (0.79±0.03, p=0.53, Fig 5A).

Interestingly, the subcellular localization of the mutant was different from WT utrn CH1-CH2 domain (Fig 5B, Fig S6 B, C). We sought to quantify differences in localization of the domains by calculating both the correlation coefficient with WT utrn ABD and by measuring the bound amounts of proteins on different actin structures (Fig 5B). The Δ-n-term Q33A T36A mutant displayed a correlation with utrn WT ABD (0.87±0.03), less than that of the control in which utrn WT ABD was imaged in both channels (0.95±0.02, Fig 5C). Sub-cellularly, this mutant was distributed more evenly on stress fibers and focal adhesions, while the native utrn ABD was comparatively more enriched in focal adhesions (Fig 5D). We speculated that the n-terminal flanking region could therefore influence subcellular localization and sought to examine the localization of native actin-binding domains with different n-terminal flanking regions. In contrast to utrophin, filamin B has a short n-terminal flanking region (Fig S6 A) and we investigated the localization of this domain in live cells (Fig S6 D). Interestingly, the WT actin-binding domain from filamin B showed preferential localization to stress fibers and was comparatively reduced at focal adhesions (Fig 5D, Fig S6 D), similar to that of the utrophin construct with n-terminal truncation with ABS1 mutations. These differences in localization were not a result of broad differences in dynamics of the proteins (as measured by Fluorescence Recovery After Photobleaching (FRAP), supplementary materials and methods, Fig S 7A), indicating a specificity for different actin structures independent of large-scale differences in actin-binding affinity.

Despite high sequence similarity and a conserved structural fold, minimal tandem calponin homology domains found in actin-binding proteins can vary in their affinity to f-actin and their localization to specific actin filament structures, which we refer to as specificity. Our work identifies new regions of CH1-CH2 binding domains that modulate affinity to actin and, surprisingly, reveals differences in specificity to filaments in actin structures. These two factors can be modified through two distinct mechanisms – CH1 to CH2 interactions for affinity, and n-terminal-CH1 to actin interactions for specificity. Each of these can be independently altered to tune the actin-binding properties of calponin homology domains (Fig 6).

Interdomain interactions are paramount for determining tandem CH domain binding affinity to f-actin. Many actin-binding diseases where CH1-CH2 domains exhibit a gain-of-function (increased actin-binding affinity) are associated with the disruption of a key salt bridge that holds the two globular CH domains in a compact configuration. Disruption of this salt bridge in our experiments increased the binding affinity of plectin to be more similar to that of utrophin, which appears to reside in an ‘open’ configuration(27). Interestingly, utrophin could be made to adopt an even more ‘open’ configuration by modifying regions outside of the well-characterized salt bridge(33), and hence increase its binding affinity. Firstly, we have shown that the interdomain linker region can impact binding affinity, by making chimeras of utrophins CH domains with the linker region from filamin A. By introducing the unstructured linker from filamin A, the CH2 can presumably move away freely from actin reducing any possible steric interactions with the filament, consistent with the large Rg observed in our SAXS measurements. This result is also consistent with previous observations that show that

even though utrophin resides in a relatively open conformation, it still undergoes a conformational change when binding to f-actin(27). Furthermore, mutations to the linker region of WT utrn ABD that are predicted to destabilize its structure (Fig S1) had a similar behavior to the filamin linker-utrophin chimera when expressed in HeLa cells (Fig S4 D), as did the chimera between utrophin CH domains and the linker region from plectin ABD (Fig S4 E). Secondly, we have shown that residues on CH domains which reside at the inter CH domain interface are also important for regulating binding affinity. We have shown that the mutations Q33A T36A on utrn ABD increases actin-binding affinity by both modulating CH1-CH2 interactions and increasing the overall flexibility of the domain, as measured by SAXS. This result contrasts with similar mutations in α-actinin-4 that have been suggested to decrease actin-binding, albeit with the full length protein(10). One possible explanation is that interactions between the mutated CH domains of α-actinin and other segments of the full-length protein exist which could have an additional role(35). Moreover, our results are consistent with a high-resolution structure for the mutant actin-binding-binding domain of filamin A E254K bound to f-actin(33). This structure is based on the open conformation of the CH1-CH2 which enables high affinity binding to actin (E254K). In this structure, ABS1 is not predicted to interact with actin. Our data, which indicates that ABS1 is primarily involved in CH1-CH2 interactions and not direct f-actin contact, is in agreement with this model(23, 33).

Through our work and others, the role of ABS1-3 has been called in to question. The initial identification of ABS 1-3 on CH domains were made with minimal peptides before CH domain crystal structures were reported. However, certain residues within these peptides may not have access to f-actin in their folded states(23). In support of this notion, the isolated CH2 domain in our studies was largely cytoplasmic, suggesting that ABS3 also does not play a significant role in directly binding to actin. Together, these results indicate that several residues outside of the well characterized interdomain salt bridge, including those in ABS1 and 3, are important for CH1-CH2 interactions, impact the configuration of the domain, and hence overall actin-binding affinity – and yet do not contact f-actin directly. Overall, our data suggest a range of 'open-ness' of CH1-CH2, which gives rise to the broad range of affinities that are observed in native CH1-CH2 domains and in disease-associated mutations. Thirdly, we have shown that the steric interaction between the CH2 and f-actin that reduces binding affinity can be modulated by adding size to this domain. By conjugating a biochemically inert PEG molecule (Rg~1nm) to the CH2 domain, we show that overall affinity of the domain is reduced ~5 fold. Interestingly, this strategy could present a potential therapeutic approach for diseases that result in gain of actin-binding function of these domains, where a binding molecule could be added to the CH2 in order to reduce binding affinity.

Finally, we observed that subtle differences in the interaction of CH1 and the n-terminal flanking region with actin filaments appear to contribute to the binding of specific actin structures. By truncating the n-terminal region of utrophin, we observed a large decrease in binding affinity, consistent with previous studies(34). However, when we introduced mutations that affect CH1-CH2 interactions, we observed that actin-binding affinity was restored – but a different localization was observed (Fig S6).

The change in localization was not the result of kinetic differences in binding, which have been proposed for the localization of myosin to the rear of migratory cells(36), as the kinetics of both actin-binding domains were similar when measured by FRAP (Fig S6 A). Importantly, this finding implies that tandem CH domains can target different actin structures and play an important, non-redundant role in spatial organization of the cytoskeleton. Given that differences in the n-terminal region vary significantly between CH domain proteins, both in sequence and length, this region is likely to have an underappreciated role in actin-binding and subcellular protein targeting. In particular, the actin-binding domain of filamin B had a similar localization to our n-terminal utrophin truncation construct (Fig S6). The n-terminal flanking region of filamin B is short, implying that the length of this region could play an important role in determining specificity to different actin structures. Interestingly, the isoforms filamin A and filamin B have high sequence similarity in the actin-binding domain but different lengths of the n-terminal flanking region (Fig S6 A). When we express the actin-binding domains from different filamin isoforms in live cells we observe different binding characteristics (Fig S6 B). A chimera of the filamin A n-terminal region, with the CH domains from filamin B partly restored localization to focal adhesions (Fig S6), but some differences in localization could still be observed in the image difference maps (Fig S6 E). This result implies that the n-terminal flanking region is indeed important for localization of the domain but is not the only factor. Future work will be required to fully investigate the role that other regions with sequence diversity have on localization.

Taken together, these data show that there are multiple modes for regulating the binding affinity of CH1-CH2 domains: interdomain interactions through salt bridges and linkers, CH2-actin steric clashes based on domain size, and CH1-actin-binding (which includes the n-terminal flanking region, Fig 6). Each of these has significance for cytoskeletal homeostasis, for targeting of actin-binding proteins to specific structures, and potentially for the development of therapeutic strategies. While CH1-CH2 domains from different proteins share similarities in structure and sequence, small differences can be significant. They can determine both binding affinity and localization and highlight why disease-associated point mutations can have such a detrimental impact.

Materials and Methods

For additional methods see supplementary methods section (*generation of cell lines, protein purification, Spinning disc confocal imaging, FRAP, CD and melting temperature measurements, SAXS, Actin filament binding assay*).

Cell Culture: HeLa and HEK293T cells were cultured at 37°C in an atmosphere of 5% CO_2 in air in DMEM (Life Tech, #10566024) supplemented with 10% FBS (Life Tech, #16140071) and 1% Penicillin-Streptomycin (Life Tech, #15140122). HEK293T cells were passaged using 0.05% trypsin and HeLa cells with 0.25% trypsin.

Relative bound fraction measurements and image difference mapping: A custom-written MatLab routine was used to calculate the relative bound fractions of different actin-binding domains, the difference maps and correlation coefficients. Briefly, images of cells expressing GFP-utrn were thresholded and binarized to generate masks of the whole cell and actin cytoskeleton. Holes within the binary image mask were filled and this was used as an outline of the cell footprint. To generate a mask for the unbound fraction the complementary image of the actin mask was taken, which included pixels only within the cell footprint (Fig 1C). Average pixel intensity measurements ($\bar{I}$) were then made using the two masks and the relative bound amount calculated from the following equation $RBF = \frac{\bar{I}_{bound} - \bar{I}_{unbound}}{1/_2(\bar{I}_{bound} + \bar{I}_{unbound})}$. In some instances of very low binding, *RBF* was less than zero. This arises due to the geometry of the cell where higher intensities are gathered from the cell body where there is more cytoplasmic signal, in comparison to actin rich regions that are often thin and flat. *RBF* is a convenient and relative measure when averaging over many cells to rule out large contributions from cell geometry or f-actin abundance. For comparing the localization of different actin-binding domains, the same masking method was used to make measurements of intensity of the CH1-CH2 of interest and utrn ABD. The images were normalized to their maximum value and the utrn ABD image values subtracted from the CH1-CH2 image to give the difference map (Fig 5B). Pearson's correlation coefficient was calculated from the image values to quantify whole cell differences in localization. To measure the relative amounts of protein bound to different actin structures (cytoplasmic, on stress fibers, and on focal adhesions), local pixel value measurements were made and normalized with the following equation $I_{Stress\ Fiber(norm)} = \frac{I_{Stress\ Fiber}}{I_{cytoplasm} + I_{Stress\ Fiber} + I_{Focal\ Adhesion}}$.

Acknowledgements

The authors would like to thank Dyche Mullins, Hengameh Shams and members of the Fletcher lab for helpful discussions. This work was supported by grants from NIH (D.A.F). A.R.H. was in receipt of an EMBO long-term fellowship 1075–2013 and HFSP fellowship LT000712/2014. B.B. was supported by the Ruth L. Kirschstein NRSA fellowship from the NIH (1F32GM115091). P.J was supported by an NSF Fellowship and the Berkeley Fellowship for Graduate Studies. A.B. was supported by the Miller Institute for Basic Research at UC Berkeley as a Miller Visiting Professor. The authors acknowledge the use of the Molecular Imaging Center core facility at UC Berkeley, and the help of the Marqusee Lab with the CD and melting temperature experiments. SAXS data was collected at SIBYLS beamline 12.3.1 at the Advanced Light Source (ALS). SAXS data collection at SIBYLS is funded through DOE BER Integrated Diffraction Analysis Technologies (IDAT) program and NIGMS grant P30 GM124169-01, ALS-ENABLE. D.A.F. is a Chan Zuckerberg Biohub Investigator.

References

1. Harris AR, Jreij P, Fletcher DA (2018) Mechanotransduction by the Actin Cytoskeleton: Converting Mechanical Stimuli into Biochemical Signals. *Annu Rev Biophys* 47:617–631.

2. Michelot A, Drubin DG (2011) Building distinct actin filament networks in a common cytoplasm. *Curr Biol* 21(14):R560–R569.

3. Korenbaum E, Rivero F (2002) Calponin homology domains at a glance. *J Cell Sci* 115(18):3543–3545.

4. Bañuelos S, Saraste M, Carugo KD (1998) Structural comparisons of calponin homology domains: implications for actin binding. *Structure* 6(11):1419–1431.

5. Gimona M, Djinovic-Carugo K, Kranewitter WJ, Winder SJ (2002) Functional plasticity of CH domains. *FEBS Lett* 513(1):98–106.

6. Winder SJ, et al. (1995) Utrophin actin binding domain: analysis of actin binding and cellular targeting. *J Cell Sci* 108(1):63–71.

7. Lee SH, Weins A, Hayes DB, Pollak MR, Dominguez R (2008) Crystal structure of the actin-binding domain of α-actinin-4 Lys255Glu mutant implicated in focal segmental Glomerulosclerosis. *J Mol Biol* 376(2):317–324.

8. Ruskamo S, Ylänne J (2009) Structure of the human filamin A actin-binding domain. *Acta Crystallogr D Biol Crystallogr* 65(11):1217–1221.

9. Sawyer GM, Clark AR, Robertson SP, Sutherland-Smith AJ (2009) Disease-associated substitutions in the filamin B actin binding domain confer enhanced actin binding affinity in the absence of major structural disturbance: Insights from the crystal structures of filamin B actin binding domains. *J Mol Biol* 390(5):1030–1047.

10. Weins A, et al. (2007) Disease-associated mutant α-actinin-4 reveals a mechanism for regulating its F-actin-binding affinity. *Proc Natl Acad Sci* 104(41):16080–16085.

11. Ehrlicher AJ, et al. (2015) Alpha-actinin binding kinetics modulate cellular dynamics and force generation. *Proc Natl Acad Sci* 112(21):6619–6624.

12. Clark AR, Sawyer GM, Robertson SP, Sutherland-Smith AJ (2009) Skeletal dysplasias due to filamin A mutations result from a gain-of-function mechanism distinct from allelic neurological disorders. *Hum Mol Genet* 18(24):4791–4800.

13. Krakow D, et al. (2004) Mutations in the gene encoding filamin B disrupt vertebral segmentation, joint formation and skeletogenesis. *Nat Genet* 36(4):405.

14. Parrini E, et al. (2006) Periventricular heterotopia: phenotypic heterogeneity and correlation with Filamin A mutations. *Brain* 129(7):1892–1906.

15. Norwood FL, Sutherland-Smith AJ, Keep NH, Kendrick-Jones J (2000) The structure of the N-terminal actin-binding domain of human dystrophin and how mutations in this domain may cause Duchenne or Becker muscular dystrophy. *Structure* 8(5):481–491.

16. Duff RM, et al. (2011) Mutations in the N-terminal actin-binding domain of filamin C cause a distal myopathy. *Am J Hum Genet* 88(6):729–740.

17. Avery AW, Thomas DD, Hays TS (2017) β-III-spectrin spinocerebellar ataxia type 5 mutation reveals a dominant cytoskeletal mechanism that underlies dendritic arborization. *Proc Natl Acad Sci*:201707108.

18. Fletcher DA, Mullins RD (2010) Cell mechanics and the cytoskeleton. *Nature* 463(7280):485–492.

19. Yao NY, et al. (2011) Nonlinear viscoelasticity of actin transiently cross-linked with mutant α-actinin-4. *J Mol Biol* 411(5):1062–1071.

20. Moeendarbary E, Harris AR (2014) Cell mechanics: principles, practices, and prospects. *Wiley Interdiscip Rev Syst Biol Med* 6(5):371–388.

21. Burkel BM, Von Dassow G, Bement WM (2007) Versatile fluorescent probes for actin filaments based on the actin-binding domain of utrophin. *Cell Motil Cytoskeleton* 64(11):822–832.

22. Singh SM, Bandi S, Winder SJ, Mallela KM (2014) The actin binding affinity of the utrophin tandem calponin-homology domain is primarily determined by its N-terminal domain. *Biochemistry* 53(11):1801–1809.

23. Galkin VE, Orlova A, Salmazo A, Djinovic-Carugo K, Egelman EH (2010) Opening of tandem calponin homology domains regulates their affinity for F-actin. *Nat Struct Mol Biol* 17(5):614–616.

24. Fealey ME, et al. (2018) Dynamics of dystrophin's actin-binding domain. *Biophys J*.

25. Keep NH, Norwood FL, Moores CA, Winder SJ, Kendrick-Jones J (1999) The 2.0 Å structure of the second calponin homology domain from the actin-binding region of the dystrophin homologue utrophin. *J Mol Biol* 285(3):1257–1264.

26. García-Alvarez B, Bobkov A, Sonnenberg A, de Pereda JM (2003) Structural and functional analysis of the actin binding domain of plectin suggests alternative mechanisms for binding to F-actin and integrin β4. *Structure* 11(6):615–625.

27. Lin AY, Prochniewicz E, James ZM, Svensson B, Thomas DD (2011) Large-scale opening of utrophin's tandem calponin homology (CH) domains upon actin binding by an induced-fit mechanism. *Proc Natl Acad Sci* 108(31):12729–12733.

28. Borrego-Diaz E, et al. (2006) Crystal structure of the actin-binding domain of α-actinin 1: Evaluating two competing actin-binding models. *J Struct Biol* 155(2):230–238.

29. Avery AW, et al. (2017) Structural basis for high-affinity actin binding revealed by a β-III-spectrin SCA5 missense mutation. *Nat Commun* 8(1):1350.

30. Singh SM, Mallela KM (2012) The N-terminal actin-binding tandem calponin-homology (CH) domain of dystrophin is in a closed conformation in solution and when bound to F-actin. *Biophys J* 103(9):1970–1978.

31. Bandi S, Singh SM, Mallela KM (2015) Interdomain linker determines primarily the structural stability of dystrophin and utrophin tandem calponin-homology domains rather than their actin-binding affinity. *Biochemistry* 54(35):5480–5488.

32. Hura GL, et al. (2009) Robust, high-throughput solution structural analyses by small angle X-ray scattering (SAXS). *Nat Methods* 6(8):606.

33. Iwamoto DV, et al. (2018) Structural basis of the filamin A actin-binding domain interaction with F-actin. *Nat Struct Mol Biol*:1.

34. Singh SM, Bandi S, Mallela KM (2017) The N-Terminal flanking region modulates the actin binding affinity of the utrophin tandem calponin-homology domain. *Biochemistry* 56(20):2627–2636.

35. Shams H, Golji J, Garakani K, Mofrad MR (2016) Dynamic regulation of α-actinin's calponin homology domains on F-actin. *Biophys J* 110(6):1444–1455.

36. Maiuri P, et al. (2015) Actin flows mediate a universal coupling between cell speed and cell persistence. *Cell* 161(2):374–386.

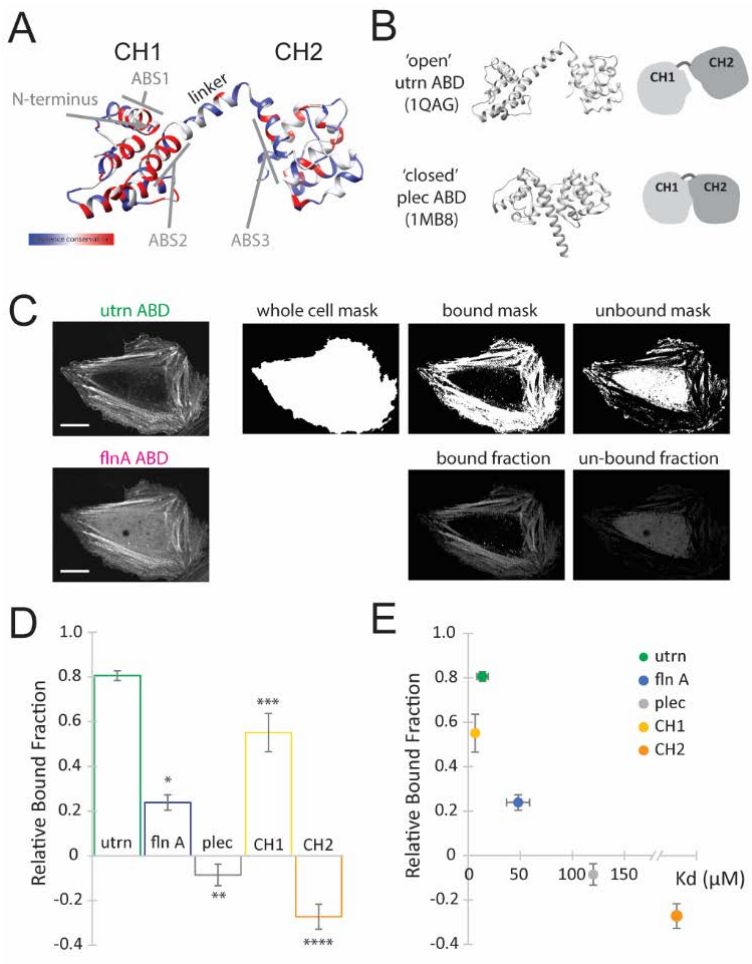

Figure 1: Measurement of bound fraction in live cells correlates with binding affinity *in vitro*

(A) Ribbon diagram of the actin-binding domain of utrophin (1QAG). Colored for sequence similarity between utrophin, filamin and plectin from blue to red. (B) Open and closed conformation of CH1-CH2 from the actin-binding domain of utrophin (1QAG, open) and the actin-binding domain of plectin (1MB8, closed). (C) Method to quantify the relative bound fraction of proteins using live cell imaging. Example images for the actin-binding domain of filamin A. The utrn channel is used to generate masks for the whole cell, for bound to actin, and for unbound protein, which are then used to calculate intensities in the CH1-CH2 channel of filamin A (bottom row, scale bar 20µm). (D) Relative bound fraction measurements compared to that from utrophin for the actin-binding domains from filamin A ($p^{*}<0.05$), plectin ($p^{**}<0.05$), CH1 from utrophin ($p^{***}<0.05$) and CH2 from utrophin ($p^{****}<0.05$). (E) Comparison of measurements of relative bound fraction in cells with *in vitro* binding affinity measurements. The Kd for CH1 = 6µM (22), the Kd for CH2 > 1000µM (22), the Kd for flnA = 47µM (8), the Kd for plectin ≈ 120µM and the Kd for utrn = 13.8µM.

.

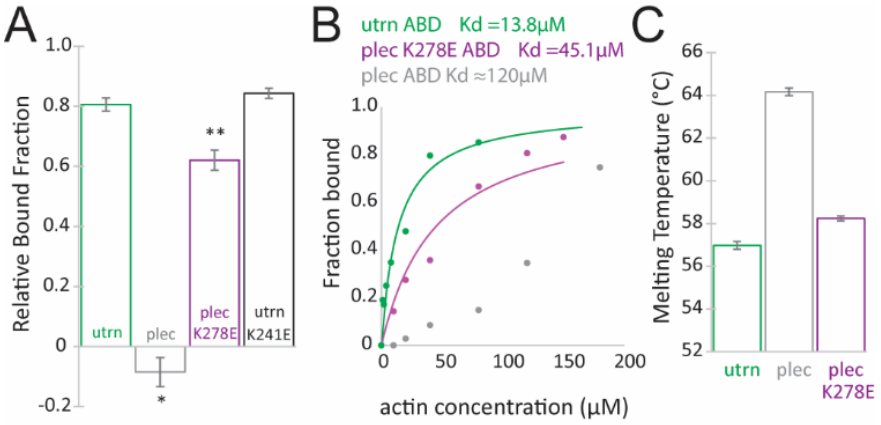

Figure 2: Binding affinity to f-actin depends on conformation and inter-CH domain salt bridge

(A) Relative bound fraction measurements for the salt bridge mutants from plectin (K278E, p**<0.05) and utrophin (K241E, p=0.07). (B) Binding curves to f-actin. Low binding is observed for plectin over the range of concentrations tested, implying a low affinity interaction. The salt bridge mutation K278E restores binding affinity. (C) Melting temperatures for the actin-binding domain of plectin and the salt-bridge mutant of plectin's actin-binding domain.

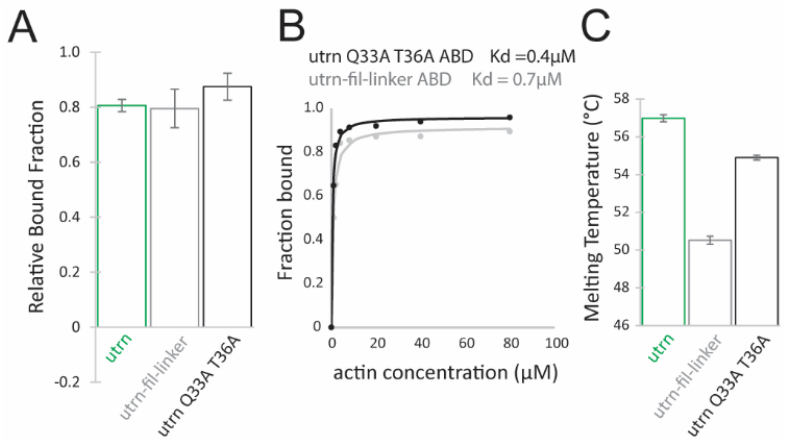

Figure 3: Mutations to the linker region or interdomain interface result in a more 'open' conformation

(A) Relative bound fraction measurements for interdomain linker (p=0.89) and interdomain interface mutants (p=0.23) of utrophin's actin-binding domain. (B) Binding curves for the two utrophin mutants show high affinity binding for the interdomain linker (Kd = 0.7μM) and interdomain interface (Kd = 0.4μM) mutants. (C) Melting temperature measurements for the interdomain linker mutant and the interdomain interface mutant of utrophin's actin-binding domain.

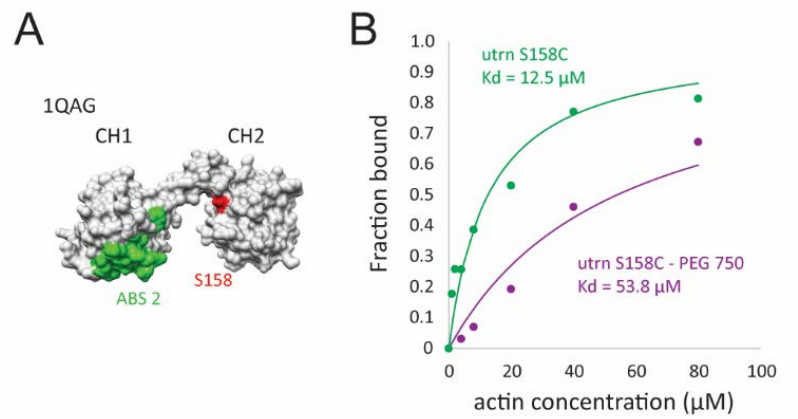

Figure 4: Binding affinity to f-actin can be reduced by increasing CH2 size
(A) Surface model of the actin-binding domain of utrophin (1QAG). The f-actin-binding surface on CH1, ABS2, is shown in green, and residue S158 on CH2 is shown in red, which was mutated to cysteine and used for PEG labelling. (B) Binding curves for the unlabeled mutant (green) and the PEG 750 Da labelled mutant (magenta). This caused a change in binding affinity from Kd=12.5µM to Kd=53.8µM.

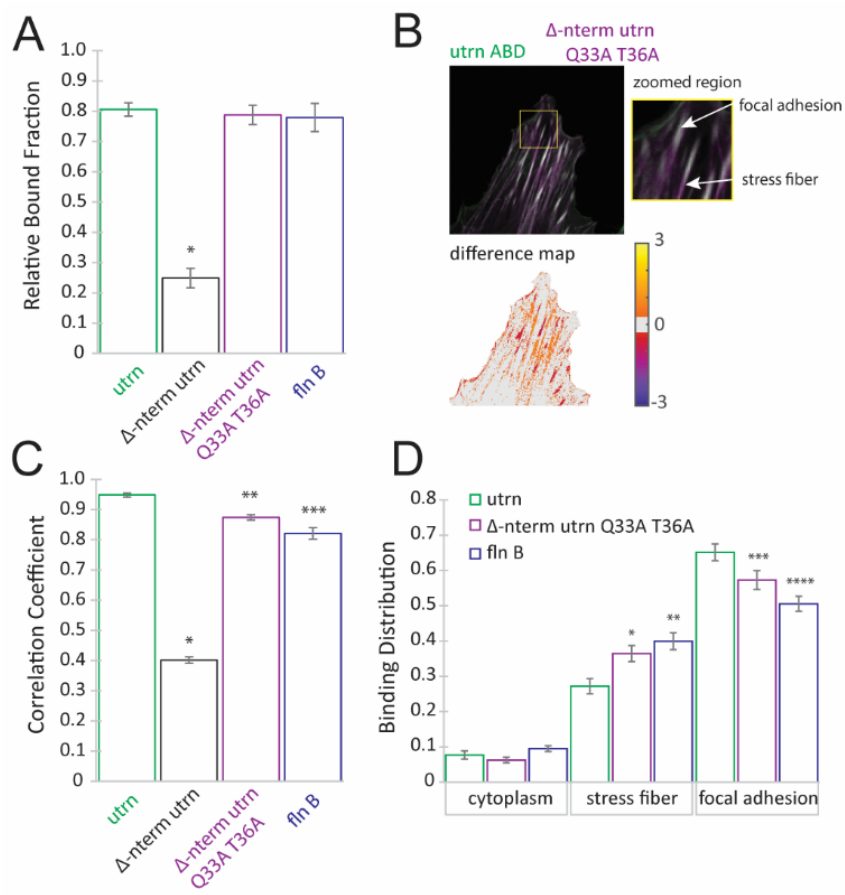

Figure 5: The n-terminal flanking region plays a role in CH1-CH2 localization to different actin structures

(A) Measurements of relative bound fraction for wild-type and n-terminal flanking region truncation constructs of utrophin's actin-binding domain (ABD). Δ-nterm utrn had a significantly lower relative bound fraction than the WT utrn ABD ($p^{*}<0.05$). (B) Subcellular localization of n-terminal truncation with additional mutations Q33A T36A, which restores binding affinity. The zoomed region shows differences in localization relative to the WT domain, which are also present in the image difference map. (C) Measurements of whole cell correlation coefficient for Δ-nterm utrn ($p^{*}<0.05$), Δ-nterm utrn Q33A T36A ($p^{**}<0.05$) and filamin B relative to WT utrn ABD. (D) Measurement of protein-binding distribution on different actin structures (cytoplasmic, on stress fibers and on focal adhesions) show significant differences in binding behaviors for both the Δ-nterm Q33A T36A construct (light grey, $p^{*}<0.05$, $p^{**}<0.05$) and the CH1-CH2 from filamin B (dark grey, $p^{***}<0.05$, $p^{****}<0.05$), implying a specificity for different actin structures.

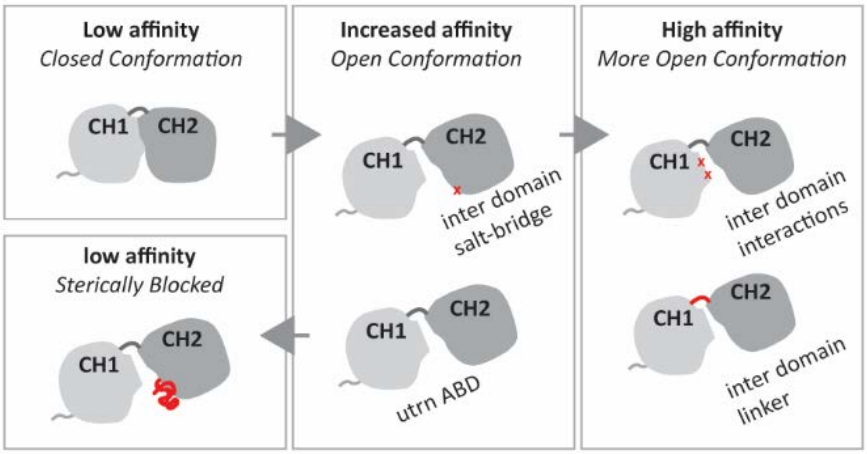

Figure 6: Tuning the affinity of Calponin Homology Domains
Low affinity binding in the closed conformation can be increased by changing the conformation to the open state. Open conformation domains can be made even higher affinity through changes to the interdomain linker region or by mutating residues at the CH1-CH2 interface. Open conformation domain affinity can be decreased by restoring the steric interaction between CH2 and actin filaments through the addition of steric bulk to the CH2 domain.